

1 **Climate change impacts on the hydrologic regime of a**
2 **Canadian river: Comparing uncertainties arising from**
3 **climate natural variability and lumped hydrological**
4 **model structures**

5

6 **G. Seiller^{1*} and F. Anctil¹**

7 [1]{Chaire de recherche EDS en prévisions et actions hydrologiques, Université Laval,
8 Département de génie civil et de génie des eaux, 1065, avenue de la Médecine, Québec,
9 Qc, G1V0A6, Canada}

10 *Corresponding author: gregory.seiller.1@ulaval.ca

11

12 **Abstract**

13 Diagnosing the impacts of climate change on water resources is a difficult task pertaining
14 to the uncertainties arising from the different modeling steps. Lumped hydrological
15 model structures contribute to this uncertainty as well as the natural climate variability,
16 illustrated by several members from the same Global Circulation Model. In this paper,
17 the hydroclimatic modeling chain consist of twenty-four potential evapotranspiration
18 formulations, twenty lumped conceptual hydrological models, and seven snowmelt
19 modules. These structures are applied on a natural Canadian sub-catchment to address
20 related uncertainties and compare them to the natural internal variability of simulated
21 climate system as depicted by five climatic members. Uncertainty in simulated
22 streamflow under current and projected climates is assessed. They rely on interannual
23 hydrographs and hydrological indicators analysis. Results show that the natural climate
24 variability is the major source of uncertainty, followed by the potential evapotranspiration
25 formulations and hydrological models. The selected snowmelt modules, however, do not
26 contribute much to the uncertainty. The analysis also illustrates that the streamflow
27 simulation over the current climate period is already conditioned by tools' selection. This

1 uncertainty is propagated to reference simulations and future projections, amplified by
2 climatic members. These findings demonstrate the importance of opting for several
3 climatic members to encompass the important uncertainty related to the climate natural
4 variability, but also of selecting multiple modeling tools to provide a trustworthy
5 diagnosis of the impacts of climate change on water resources.

6

1 **Keywords**

2 Hydrological modeling, climate change, uncertainty, intercomparison, natural variability

3

4 **1 Introduction**

5 The modeling of climate change impacts on water resources remains a major challenge
6 encompassing numerous uncertainties, from the definition of a greenhouse gas scenario
7 to the calculation of the hydrological projection. Every modeling tool involved in this
8 process can potentially affect our ability to render a precise diagnosis of the future.

9 Quantifying the uncertainties associated with the modeling of climate change impacts
10 asks for a consistent and documented approach, reflecting the state of the scientific
11 knowledge (Kiparsky and Gleick, 2004; Dettinger, 2005; Maurer, 2007). These
12 uncertainties may be separated into two components: “incomplete” knowledge, reflected
13 by model conceptualization, and “unknowable” knowledge, related to human and climate
14 system behaviors (Carter *et al.*, 1999). Among the four levels of climate change impacts
15 modeling uncertainties (Boé *et al.*, 2009), three are associated to future climate
16 calculations (gas emissions scenarios, global climate modeling, and downscaling) and
17 one, to hydrological modeling. Several studies addressed all of them (e.g. Vicuna *et al.*,
18 2007; Minville *et al.*, 2008; Kay *et al.*, 2009; Boyer *et al.*, 2010; Gørgen *et al.*, 2010;
19 Teng *et al.*, 2012; Jung *et al.*, 2012) while others focused on specific ones (e.g. Ludwig *et al.*,
20 2009; Gardner, 2009; Poulin *et al.*, 2011; Bae *et al.*, 2011; Teng *et al.*, 2012;
21 Velázquez *et al.*, 2013). However, all these works are based on ensemble intercomparison
22 and advocate the necessity of assessing uncertainties before, for example, comparing
23 river discharges over reference (REF) and future (FUT) periods.

24 For instance, Minville *et al.* (2008) found that GCMs initiate an important part of the
25 uncertainty but so does, to a lesser extent, climate downscaling and hydrological
26 modeling. Kay *et al.* (2009) arrived to similar conclusions. They compared six different
27 sources of uncertainty: gas emissions scenarization, global climate modeling (GCM),
28 climate downscaling, natural variability (which is disclosed calculating GCM runs from
29 slightly modified initial conditions), and hydrological model structures and parameters.

1 They found that all contribute to the total uncertainty and that GCMs are the most
2 uncertain. For their part, Teng *et al.* (2012) exploited fifteen GCM and operated five
3 hydrological model structures to show that the uncertainty deriving from the hydrological
4 modeling should not be disregarded. Conclusions shared by Prudhomme *et al.* (2003),
5 Vicuna *et al.* (2007), Boé *et al.* (2009), Quintana Seguí *et al.* (2010), and others.

6 Hydrologists continue improving their models, yet the role of the model structures in
7 climate change impacts studies is still little known. Intercomparison studies offer a
8 simple way of unravelling uncertainties associated to the many hydrological structures
9 and concepts. As an example, Ludwig *et al.* (2009) focused on uncertainties emanating
10 from hydrological modeling, comparing structures of different complexity. They
11 confirmed the importance of the climatic projection uncertainty (i.e. scenarios, GCM,
12 downscaling) but also stressed that hydrological modeling tools must be carefully
13 evaluated and that a coherent protocol must be developed. Poulin *et al.* (2011) identified
14 equifinal parameter sets for two hydrological structures implemented on a Canadian
15 catchment. They concluded that model structures and parameter identification are
16 important sources of uncertainty under a changing climate. Velázquez *et al.* (2013)
17 confirmed that the selection of a hydrological model affects climate change impacts
18 conclusions, especially for low flows on two dissimilar catchments, in Germany and
19 Canada.

20 Many hydrological models resort to a simplistic approach to simulate the actual
21 evapotranspiration, namely to an agronomic concept called potential evapotranspiration
22 (PET), representative of constant crop and soil conditions. PET formulations are largely
23 influenced by a changing climate (changes in the evaporative demand) and are thus a
24 supplemental source of uncertainty. However, scant research addresses this question even
25 if the diversity of PET formulations and concepts is compatible for intercomparison. As
26 an example, Kay and Davies (2008) found that Penman equation compared to a simple
27 temperature-based formulation (Oudin *et al.*, 2005) in a climate change context with A2
28 scenario, both offer very different results for climate change impacts modeling on water
29 resources for the 2071-2100 period. They advised that the choice of a PET formulation
30 affects hydrological projections. Bae *et al.* (2011) evaluated uncertainties from

1 hydrological models and PET formulations on a Korean catchment. They compared three
2 hydrological models, three PET formulations, and thirty-nine climate scenarios for the
3 2020 and 2080 horizons. Their results showed that hydrological modeling affects total
4 uncertainty, revealing the importance of the PET formulation and demonstrating the need
5 to account for them in climate change impacts assessment projects. More, Bormann
6 (2011) compared eighteen PET computations over six German meteorological stations
7 and found a large sensitivity to climate.

8 The authors are aware of no work addressing the hydrological projections uncertainty
9 emanating from lumped snow modules, but the literature targeting snow melt modeling
10 (e.g. WMO, 1986; Valéry, 2010, Franz *et al.*, 2010) reported large uncertainties on the
11 simulated discharge. It is thus expected that this variability remains at least as important
12 under changing climate.

13 In this work, PET formulations, snow modules, and lumped hydrological structures are
14 compared, along with the natural variability of the simulated climate system. This later
15 concept is illustrated here with a climatic ensemble based on five members with slightly
16 different initial conditions, such as in Deser *et al.* (2012), where the natural climate
17 variability refers to the “unforced variability internal to the real or simulated climate
18 system” as evaluated with 40 members. Climate simulation ensembles allow the analysis
19 of their internal variability (which is mainly a demonstration of natural variability) and
20 can be seen as the irreducible fraction of climate simulations uncertainty (Kay *et al.*,
21 2009, Velázquez *et al.*, 2013), a part of the “unknowable” knowledge stated above.
22 Climatic reference simulations (REF) and future projections (FUT) may then vary
23 substantially from one member of the ensemble to the other. Indeed, the chaotic nature of
24 the climate produces dissimilar time series when a GCM is initiated with slightly
25 modified conditions, here in 1850. The natural climate uncertainty, described by equally
26 valid climatic members (C1 to C5), will thus serve as benchmark for the other explored
27 sources of uncertainty.

28 More specifically, this project compares uncertainties related to the natural climate
29 variability and to lumped hydrological model structures, in the context of climate change
30 impacts on the hydrologic regime of a Canadian river. It will illustrate what is our ability

1 to produce a diagnosis of climate change impacts on the water resources of the *au*
2 *Saumon* catchment.

3

4 **2 Material and methods**

5 **2.1 The *au Saumon* catchment**

6 The *Haut-Saint-François* catchment drains a 2940 km² territory located 120 km south of
7 Quebec City and 200 km east of Montreal. It fosters three dams for flood control,
8 environmental needs, recreational activities, and water consumption – the lower one is
9 mostly dedicated to hydroelectric production. The natural *au Saumon* (SAU) sub-
10 catchment, upstream the *Haut-Saint-François* River, receives waters from a 738 km² area
11 along a south/south-east to north/north-west path. Figure 1 details this location and its
12 geographic characteristics. The hydrographic network is dense and uniformly distributed,
13 altitudes range from 277 m and 1092 m, land use is dominated by mixed
14 coniferous/deciduous forests and agricultural lands, while the geology is dominated by
15 limestone, sandstone, and shale. The hydrologic regime is characterized by an important
16 spring freshet (from March to May) and high autumnal flows.

17 **2.2 Hydrological, meteorological and climatic data**

18 Hydrological and meteorological data are provided by the *Centre d'expertise hydrique du*
19 *Québec*. Hydrometrical data correspond to daily discharges from the *au Saumon* gauging
20 station (1975 to 2003). The annual mean discharge reaches 771 mm (approximately 18
21 m³/s on an average day).

22 Meteorological observations consist in daily mean, minimum and maximum air
23 temperatures (°C), daily total precipitation (mm), incoming solar radiation (W/m²),
24 relative humidity (%), and wind speed at 2 m (m/s). Radiation, humidity and wind speed
25 measurements originate from the nearby Sherbrooke station, outside of the watershed. All
26 data are spatially lumped over the catchment and extend from 1975 to 2003. Mean
27 temperature attains 4.5 °C but only -11 °C in January. Precipitation is quite uniform over

1 the year and averages 1284 mm, with 355 mm as solid precipitation. Maximal incoming
2 solar radiation occurs in June (246 W/m^2) while the relative daily humidity fluctuates
3 between 73% (April) and 85% (September). Average wind oscillates from 2 m/s (August)
4 to 3.5 m/s (March).

5 Climatic data originated from the Canadian Global Climate Model (CGCM version 3
6 with a 3.75° resolution, Scinocca *et al.*, 2008), fed with SRES A2 scenario (Nakicenovic
7 *et al.*, 2000). Data were dynamically downscaled by the Canadian Regional Climate
8 Model (CRCM version 4.2.3, de Elía and Côté, 2010). The CRCM domain consisted of
9 111×87 grid points with a 45 km resolution (true at 60°N) centered on the Province of
10 Quebec.

11 Downscaled climatic data were provided by Consortium Ouranos: reference simulations
12 (REF) cover 1971 to 2000 while future projections (FUT), 2041 to 2070 (2050s horizon).
13 The climate natural variability is depicted by five climatic members (C1 to C5) that were
14 bias-corrected to reduce deviation between REF and observations on precipitation and
15 temperature. Monthly correction factors were computed for each climatic member on the
16 30-years monthly average minimum and maximum temperatures and were applied on
17 each member to preserve their respective variance. Precipitation was corrected using the
18 LOCAL Intensity (LOCI) scaling method (Schmidli *et al.*, 2006), adjusting mean monthly
19 precipitation in terms of frequencies and intensity over 30 years. This procedure assumes
20 that these corrections are maintained in future climate. Monthly average FUT temperature
21 time series increase between 2 and 3 $^\circ\text{C}$, without much variability between climatic
22 members. Precipitation highlights a larger variability than temperature, from one climatic
23 member to the other. Projected precipitation changes are substantial, increasing mostly
24 from October to May and decreasing in summer. Incoming solar radiation slightly
25 increases on FUT from June to August and relative humidity is mostly unchanged, with a
26 small increase in March. Wind speed slightly increases in FUT (maximum + 0.8 m/s).

27 **2.3 Hydroclimatic modeling chain**

28 The main objective of this intercomparison consists in evaluating multiple representations
29 of hydrological modeling behaviors, beyond the pre-supposed most appropriate model,

1 because models are conceptualisations of real systems. It would then be possible to
2 evaluate and quantify structural uncertainties in a climate change context. The issue is to
3 select relevant hydrological modeling tools in terms of number, diversity and pertinence,
4 since they must be hypothetically appropriate for simulating catchment flows and must be
5 known for their performance.

6 **2.3.1 Twenty lumped conceptual hydrological models**

7 Researches led by Perrin *et al.* (2001, 2003) and by Mathevet (2005) provide a hefty
8 source of information on lumped conceptual hydrological models. It concerns a large
9 number of rainfall-runoff structures, tested on numerous watersheds, exploiting diverse
10 rainfall-runoff transformation concepts and soil moisture accounting processes (e.g.
11 linear, non-linear, multilayer, etc.). They are also designed to take into account many
12 contributions to the total flow, based on storages (also called buckets) and
13 interconnections, as well as flow routing delay (e.g. unit hydrogram, time lags, etc.). In
14 some cases, when the sensitivity was considered small, their designers have fixed some
15 of their parameters in order to favour the parsimony of the models, reducing computation
16 time and equifinality issues. These models, or part of, were exploited by Velázquez *et al.*
17 (2010) for exploring multimodel ensemble forecasting and by Seiller *et al.* (2012) for
18 assessing the robustness of the ensemble under contrasted climate.

19 Twenty conceptual lumped hydrological models (M01 to M20) were tested (see Table 1).
20 They rely on four to ten free parameters and on two to seven storages – the number of
21 storages correspond to the ones structuring the model and consequently they do not all
22 participate directly to the routing. In the same way, it was recognised that interception
23 function can be assimilated as a “surface storage”. Figure 2 illustrates the structural
24 diversity of the selected models. It informs on their inputs and output, as well as on the
25 different types of storages: surface, soil, root zone, groundwater, main routing, delayed
26 routing, etc. All models were applied in exactly the same conditions and run at a daily
27 time step.

1 **2.3.2 Twenty-four potential evapotranspiration formulations**

2 Oudin *et al.* (2005) and Xu and Singh (1997, 1998, 2000, 2001, 2002) provided a great
3 source of inspiration for PET formulation selection. For instance, Oudin *et al.* (2005)
4 implemented 27 PET formulations and four hydrological models on 308 catchments of
5 diverse hydroclimatic conditions.

6 Twenty-four PET formulations (E01 to E24), adapted to our hydroclimatic context, were
7 selected for this study. They are of three types: combinational (six), temperature-based
8 (eight), and radiation-based (ten). Table 2 lists the formulas and related input data.
9 Classification into families depends on the development philosophy more than their input
10 data. For example, Priestley-Taylor formula (E04) is combinational even if wind speed is
11 not explicitly used as an input, because it is a simplification of Penman formula (E01).
12 On the opposite, Doorenbos-Pruitt formula (E20) is an adaptation of radiation-based
13 formula E22 (Makkink), even if wind speed is used as an input data. All of them originate
14 from various regional contexts and development objectives, but our selection aims to
15 cover a large spectrum of concepts in order to favour diversity.

16 Empirical coefficients have been set for the *au Saumon* catchment, based on recent
17 developments and applications. Shared parameters or variables have been computed
18 based on EWRI-ASCE report recommendations (Allen *et al.*, 2005).

19 **2.3.3 Seven snow modules**

20 Valéry (2010) studied existing snow modules from a hydrological (streamflow) point of
21 view, before proposing a novel one: CemaNeige. The latter originates from a
22 comprehensive database composed of 380 watersheds exposed to diverse Nordic
23 meteorological and geographical conditions in Sweden, France, Canada, and Switzerland.
24 Parsimony, performance and robustness were the main objectives of the CemaNeige
25 development.

26 The degree-day based CemaNeige (Valéry, 2010; Nicolle *et al.*, 2011) relies on two free-
27 parameters: K_f , the melting rate ($\text{mm}/^\circ\text{C}$) and C_{Tg} , the snowpack thermal state coefficient
28 (no unit), and on two state variables: G , the snowpack in mm and eTg , the snowpack
29 thermal state in $^\circ\text{C}$. CemaNeige exploits five altitudinal layers of equal area. Its

1 precipitation partition, between solid and liquid, can be computed by two different
2 formulations, depending on the layer altitude. Liquid precipitation is directly by-passed to
3 the hydrological model, whereas solid precipitation is cumulated in the snowpack G. The
4 thermal state of the snowpack is calculated with air temperature and C_{Tg} coefficient. Melt
5 depends on degree-day and is only activated when temperature is above the melt
6 temperature (fixed at 0 °C) and depending on the K_f parameter. Effective melt (mm/day)
7 is inputted to the hydrological model.

8 Valéry's thesis details the many concepts and structures considered during the
9 development process of CemaNeige (N1). Inspired by a parsimonious bottom-up point of
10 view, a concept or structure was only retained in CemaNeige if it substantially improved
11 the hydrological performance over most of the 380 tested watersheds. It is thus opted in
12 the present study to explore some of these rejected concepts, functions, and parameters in
13 order to develop six alternative snow modules (N2 to N7) of various structural levels of
14 complexity. Individual concepts (i.e. air temperature, melt temperature, precipitation
15 separation, melting rate, melt weighting, altitudinal layering, thermal state, melt routing,
16 precipitation correction, liquid water retention, and heat due to rain) were compared in
17 order to compile the six new versions (see Figure 3 and Table 3). Selection is a
18 compromise between performance (close or above CemaNeige' ones for the *au Saumon*
19 catchment) and internal diversity (snowpack, solid precipitations, thermal state, and
20 effective melt).

21 **2.4 Model calibration**

22 Hydrological models calibration is achieved over the entire observed dataset (i.e. from
23 1975 to 2003) – differential split sample tests were performed in Seiller *et al.* (2012). It
24 relies on the Shuffled Complex Evolution (SCE) algorithm (Duan and Gupta, 1992; Duan
25 *et al.* 1994), a robust heuristic automatic optimisation tool (error minimisation) that is
26 common in hydrological sciences and is known for its performance (e.g. Wang *et al.*,
27 2009). The SCE proceeds in five steps over the entire parametric space by generating an
28 initial parameter population, ranking results, partitioning into complexes, evolving
29 complexes, and recombining them until the convergence criteria is reached. Here, the

1 objective function is the Nash-Sutcliffe efficiency (Nash and Sutcliffe, 1970) computed
2 on root-squared discharges (NSE_{sqrt}):

$$3 \quad NSE_{\text{sqrt}} = 1 - \frac{\sum_{i=1}^N \left(\sqrt{Q_{\text{sim},i}} - \sqrt{Q_{\text{obs},i}} \right)^2}{\sum_{i=1}^N \left(\sqrt{Q_{\text{obs},i}} - \sqrt{Q_{\text{obs}}} \right)^2} \quad (1)$$

4 with $Q_{\text{obs},i}$ and $Q_{\text{sim},i}$ respectively the observed and simulated discharges at time step i and
5 N the total number of observations. Criteria on root-squared discharges are considered as
6 multi-purpose, evaluating global deviation between observed and simulated discharges
7 with a lesser emphasis on high flow discharges than the standard NSE on non-
8 transformed discharges (Chiew and McMahon, 1994; Oudin *et al.*, 2006).

9 3360 calibrated parameter sets (i.e. one for each hydrological model/PET/snow module
10 combination) are then available for reference simulations (REF, 1970-2000) and future
11 projections (FUT, 2041-2070). Such methodology assumes that the parameter sets are
12 compatible for current and future climatic conditions, addressing the issue of
13 transposability. Transposability in time, on contrasted climatic conditions, is discussed
14 for the same catchment and models in Seiller *et al.* (2012).

15 **2.5 Uncertainty assessment of hydroclimatic simulations and** 16 **projections**

17 Current simulations (or calibration, CAL), reference simulations (REF) and future
18 projections (FUT) consist in a large number of time series. They exploit the 3360
19 parameter sets, which lead to:

- 20 - 3360 simulations (20M x 24E x 7N) for the observed period
- 21 - 16800 simulations (20M x 24E x 7N x 5C) for the reference period
- 22 - 16800 projections (20M x 24E x 7Nx 5C) for the future period

23 After the appraisal of the calibration performance on the Nash-Sutcliffe efficiency, to
24 illustrate the effects of modeling tools selection on the calibration process, an uncertainty

1 assessment is performed mainly based on these simulated and projected hydrographs and
2 resulting hydrological indicators (overall mean flow, OMF).

3 Cumulative streamflow uncertainty is evaluated first, representing the total uncertainty
4 including hydrological models, PET formulations, snow modules, and climatic members.
5 This step is performed on the CAL period where the measured discharges are available
6 and then on REF and FUT periods to illustrate if this uncertainty varies with the
7 simulated or projected period with climatic inputs.

8 More, on the CAL period, it may be helpful to explore the reliability of the quantiles'
9 envelopes, empirically drawn from the 3360 simulations, to comment if the latter can be
10 directly interpreted as confidence intervals. The concept of a confidence interval
11 reliability diagram consists in verifying if the observed relative frequency correspond to
12 the simulated one – perfect reliability would result in a 1:1 slope on the diagram (Wilks,
13 1995). Several confidence intervals are thus plotted (from 0.1 to 0.9) with, for example,
14 0.5 corresponding to the quartiles spread (25 % to 75 %) and 0.9 corresponding to the
15 spread of the 5 % to 95 % quantiles. Thus, for each of the 3360 simulations and each
16 confidence interval, statement if observed discharge is included or not is verified,
17 resulting in a reliability graph (Boucher *et al.*, 2009; Velázquez *et al.*, 2010).

18 Streamflow uncertainty is then evaluated for each modeling process (i.e. hydrological,
19 PET, snow, natural climatic variability) based on hydrological indicators, namely the
20 overall mean flow (OMF), corresponding to averaged daily flow for the entire simulation
21 period. A process-based streamflow uncertainty is then available, allowing comments
22 about its extent on the observation period and about its change from REF to FUT periods.

23 All these steps highlight the influences of climate change on water resources, but mostly
24 evaluate the uncertainty in our diagnosis, related to hydrological modeling and natural
25 internal variability of simulated climate system.

26

1 **3 Results**

2 **3.1 Calibration performance**

3 Table 4 summarises the outcome of the calibration in terms of NSE_{sqrt} for each
4 hydrological tool, providing median values and 5th and 95th percentiles (in brackets). The
5 hydrological model section (M01 to M20) pools 168 values per model, the PET
6 formulation section (E01 to E24) embeds 140 values per formulation, while the snow
7 module section (N1 to N7) groups 480 values per module. The best performance is
8 achieved by M05, with a median NSE_{sqrt} of 0.81, while M02 (0.56) and M13 (0.57) rank
9 last. E12 (0.66) is the less efficient PET formulation while E23 (0.78) is prevalent. It
10 should be highlighted that PET performance is less contrasted than for the hydrological
11 models. Snow modules are quite uniform in terms of performance (0.75), except N7 that
12 is lesser (0.71). The overall performance is quite satisfying and shows a great adequacy
13 between the observed and simulated discharge on the *au Saumon* catchment.

14 **3.2 Cumulative streamflow uncertainty**

15 **3.2.1 Observation simulation**

16 Assessment of the observation total cumulative uncertainty illustrates the diversified
17 response of our individual modeling tools on a period for which discharges are available.
18 Initial modeling miscues may thus be identified and characterised, on an interannual
19 average daily basis.

20 The cumulative uncertainty on the *au Saumon* catchment is illustrated in Figure 4: the
21 pale and dark blue envelopes illustrate the distribution of the streamflow ensemble (5 %
22 to 95% and 25 % to 75 %, respectively), the blue line, the median flow, and the black
23 line, the observed flow. Envelopes are drawn connecting daily discharges, using a
24 moving average to smoother the lines. Observations fall within the 5 % to 95 % envelope
25 except for a part of January (underestimation), a few days in September (overestimation)
26 and from mid-November to the third week of December (underestimation). The highest
27 uncertainty occurs during the most active hydrological period, namely the spring flood,

1 with a maximum spread of 2.74 mm on April 22 (between 7.15 and 4.41 mm). The
2 smallest uncertainty ensues during the winter low flows, with a minimum spread of 0.37
3 mm on February 10 (between 0.96 and 0.59 mm). These findings confirm that high flows
4 are more complex to encompass than low flows, probably because of their irregular
5 behavior. However, the choice of an objective function based on root-squared
6 transformed discharges may also provide an explanation for this specific behavior. Still, it
7 remains a relevant criterion for climate change impacts.

8 As mentioned in the material and methods section, exploration of the reliability of the
9 quantiles' envelopes, empirically drawn from the 3360 simulations, aims at commenting
10 if the latter can be directly interpreted as confidence intervals. For this purpose, a
11 confidence interval reliability diagram is computed for the *au Saumon* catchment. Results
12 in Figure 5 reveal a slight under-dispersion, confirming a possible link between the
13 envelopes drawn in Figure 4 and confidence intervals.

14 These results confirm that the ability to simulate the precipitation-runoff transformation
15 is hampered by the choice of lumped conceptual modeling tools. However, it can be
16 questioned if this uncertainty is maintained, reduced or increased with climatic data as
17 inputs and if it persists in future projections, affecting *de facto* our ability to report a
18 diagnosis of the impacts of climate change on water resources.

19 **3.2.2 Climate simulation and projection**

20 Figure 6 and Figure 7 present a similar hydrograph analysis for reference simulations
21 (REF, green) and future projections (FUT, red), respectively, based on climate data.
22 Streamflow uncertainty originates either from the hydrological modeling process or from
23 the climate natural variability (members), as disclosed by 16800 simulations and
24 projections. For REF (Figure 6), as for the observations, the largest uncertainty occurs
25 during spring flood with a maximum spread of 3.19 mm (between 7.53 and 4.34 mm) on
26 April 26, while the smallest uncertainty takes place in winter, December 27, when the
27 spread falls to 0.56 mm (between 1.29 and 0.73 mm). For FUT (Figure 7), the largest
28 uncertainty (2.86 mm) is reached on April 19, with discharge oscillating between 6.84
29 and 3.98 mm, and smallest uncertainty occurs February 1, with a 0.81 mm spread

1 (between 2.42 and 1.61 mm). REF and FUT uncertainties are more important than
2 simulation on the observed period, but the latter do not account for the climate natural
3 variability (members). Envelops are more uniform over the year, when including the
4 climate natural variability.

5 Evolution from REF to FUT reveals a spring flood arriving fifteen days earlier, with a
6 slight decrease in the spring high flows. More, changes favour an increase of winter low
7 flows and a decrease of summer low flows, demonstrating a substitution in time of the
8 lowest flows.

9 This streamflow uncertainty analysis, based on interannual hydrographs combining the
10 influence of the hydrological process and of the climate natural variability, reveals some
11 adversity in our ability to produce a clear diagnosis of climate change impacts on water
12 resources for the *au Saumon* catchment. Indeed, cumulative uncertainties envelopes are
13 large, especially on hydrologically sensitive periods such as spring high flows and
14 summer low flows.

15 **3.3 Process-based streamflow uncertainty**

16 Analysis of the cumulative uncertainty from yearly averaged hydrographs highlights the
17 extent of the uncertainty in simulation and projection, but without providing much
18 information about its origin. To assess this question in more details and to identify which
19 modeling step contributed the most to the reported cumulative uncertainty, a water
20 resources manager point of view is taken next, using a simple hydrological indicator: the
21 overall mean flow (OMF). This process-based streamflow uncertainty is then computed
22 on the observation period and on changes from REF to FUT periods.

23 **3.3.1 Observation OMF**

24 Figure 8 illustrates, by type of tools, the OMF uncertainty for simulations on the
25 observation (calibration) period – 168 values per boxplot for the lumped conceptual
26 hydrological models, 140 values per boxplot for the PET formulations, and 480 values
27 per boxplot for the snow modules – while the OMF total uncertainty shows 3360 values.
28 In Figure 8, colored bars indicate the 25 % and 75 % quartiles of each distribution, while

1 the horizontal white line identifies the median value. The latter can be associated to the
2 uncertainty for each tool, while the interquartile range (e.g. blue bars for the models) can
3 be perceived as depicting sensitivity and robustness. Finally, the observed OMF (2.12
4 mm) is illustrated by a red cross in the total uncertainty box. The latter is higher than
5 most of the 3360 runs because, as already mentioned in the hydrographs analysis, the
6 observed spring high flow is in general underestimated.

7 M04 median OMF (2.13 mm) is quite close to the observed one. It is however the highest
8 median OMF out of 20. The lowest one is the M12 median OMF (1.83 mm), disclosing
9 the range of the uncertainty emanating from the lumped conceptual models and the
10 importance of selecting the right model if exploiting only one structure. It can also be
11 pointed out that M05 and M08 generate reduced inner sensitivity (i.e. smaller
12 interquartile ranges), while the opposite is true for M12 and M07.

13 PET OMFs divulge an even higher uncertainty than for the lumped conceptual models.
14 Indeed, their median OMF range from 2.48 mm (E02) to 1.79 mm (E20), largely
15 encompassing the observed OMF (red cross), but also stressing the necessity of selecting
16 an appropriate PET formulation. The PET inner sensitivity (extent of the green bar)
17 varies also considerably from one another, the largest and smallest ranges originating
18 from E02 and E23, respectively. Note finally that some PET OMF distributions are quite
19 asymmetrical, namely for E01, E02, E03, E04, E06, and E10, combination formulations
20 for most of them.

21 If the selection of a particular lumped conceptual model and of a particular PET
22 formulation have a huge impact on the OMF uncertainty, it is clearly not the case for the
23 seven selected snow modules, which interquartile ranges and median OMFs, extending
24 from 1.96 mm (N1) to 1.95 mm (N7), are all quite similar.

25 **3.3.2 OMF relative change**

26 A similar analysis is performed on the OMF relative change from REF to FUT
27 [$100 \times (\text{OMF}_{\text{FUT}} - \text{OMF}_{\text{REF}}) / \text{OMF}_{\text{REF}}$, in %], drawing boxplots (Figure 9) for each modeling
28 process and for each climatic member (red), the latter in order to depict the climate
29 natural variability – each member originated from the same GCM initiated with slightly

1 modified initial conditions in 1850, expressing the chaotic nature of the climate. Total
2 OMF uncertainty then combines 16800 relative changes, 840 ones per lumped conceptual
3 model, 700 per PET formulation, 2400 per snow module, and finally 3360 per climatic
4 member. Focus is again mainly given to median values (uncertainty) and interquartile
5 ranges (inner sensitivity).

6 The total OMF relative change fluctuates from -11 % to + 129 %, but its interquartile
7 range is restrained from +4.2 % to +16.2 %, with a median value of +9.3 %. This total
8 uncertainty is distributed between conceptual hydrological modeling tools (namely PET,
9 hydrological models, and snow modules) and climatic members.

10 The median OMF relative change per lumped conceptual model fluctuates from +6.3 %
11 (M02) to +16.8 % (M08), confirming the sensitivity to the lumped conceptual model
12 selection. The interquartile range is more uniform from one model to the other than in
13 Figure 8, but M08 differs (18.1 %) in that regard – M08 was already identified with poor
14 transposability on the same catchment by Seiller *et al.* (2012). The lowest inner
15 sensitivity is achieved by M11 (10.9 %). PET OMF relative change is in general slightly
16 higher than for the lumped conceptual models, from +4.1 % (E13) to +17.1 % (E21),
17 stressing also the sensitivity to the selection of a PET formulation. The highest
18 interquartile range is obtained by E21 (14.5 %), and the lowest by E02 (10.6 %). Again,
19 the behaviour of the snow modules is more uniform than for the lumped conceptual
20 models and for the PET formulations. The median OMF relative change of the snow
21 modules are limited from +9.1 % (N2) to +9.9 % (N3), while their interquartile ranges
22 vary from 12.5 % (N3) to 11.9% (N2).

23 On the other hand, the behaviour of the climatic members is quite distinct. First, the
24 interquartile ranges of their OMF relative change are much reduced when compared to
25 the others: from 4.8 % (C1) to 3.6% (C4), expressing lower inner sensitivity. Second,
26 their median OMF relative changes vary considerably: between +2.7 % (C4) and +19.1 %
27 (C3). This latter characteristic exemplifies the importance of the climatic natural
28 variability. Changes differ greatly from one climatic member to the other. It is thus
29 evident that a single 30-year realisation of the climate is insufficient to depict all the
30 possible variability. Furthermore, it is also striking that an important part of the

1 uncertainty spread revealed by the various hydrological processes actually originates
2 from the climatic natural variability.

3 The example of this application to the *au Saumon* catchment demonstrates the limit of
4 our ability to provide a clear diagnosis of climate change impacts on water resources,
5 especially when looking at the total OMF relative change, combining 16800 simulations
6 and projections. From these results, climatic natural variability is the first uncertainty
7 driver, followed by PET formulations, lumped conceptual models, and snow modules, as
8 depicted by the standard deviations of the median OMF relative change (Table 5), with
9 respective values of 6.9 %, 3.3 %, 2.4 %, and 0.3 %.

10 Since snow accumulation and melt are important hydrological processes on the *au*
11 *Saumon* catchment, standard deviations of the median OMF relative change are also
12 provided in Table 5 distinguishing months with mean interannual air temperature above
13 0°C (April to October) from months with mean interannual air temperature below 0°C
14 (November to May). This distinction has only a small influence on the respective
15 standard deviation values and none on the ranking of the uncertainty sources.

16

17 **4 Discussion and conclusion**

18 This paper explored uncertainties related to the hydrological modeling of climate change
19 impacts on water resources. In particular, twenty lumped conceptual hydrological
20 models, twenty-four PET formulations, and seven snow modules were assessed in order
21 to evaluate our skill diagnosing the impacts of climate change on the hydrologic regime
22 of a river. Natural climate variability, through climatic members, was also studied for
23 comparison with the diverse hydrological structures.

24 Analysis on uncertainties illustrates that streamflow simulation over the current climate
25 period (calibration) is already largely conditioned by hydrological tools' selection,
26 propagating this uncertainty on reference simulation and future projection. Results
27 indicate that the largest source of uncertainty is associated to the natural climate
28 variability, followed by PET formulations, lumped conceptual models, and snow
29 modules. Calibration process and transposability questions thus appear as major issues

1 for the calculation of future hydrological projections, but natural variability plays an even
2 more substantial role in our ability to provide a diagnosis on the impacts of climate
3 change on the hydrologic regime of a river, especially when exploiting hydrological
4 indicators such as the OMF. Nonetheless, the fact that changes in the hydrologic regime
5 of the *au Saumon* catchment differed greatly from one climatic member to the other; one
6 has to question if a single 30-year realisation of the climate is sufficient to encompass all
7 the possible variability.

8 This work focussed on only one Canadian catchment and must be confirmed with other
9 watersheds and climate contexts, but the proposed methodology is easily transferable.
10 Following climate natural variability, PET formulations add to the total uncertainty in a
11 substantial way, but without much distinction between combinational, radiation-based,
12 and temperature-based formulations. It must be acknowledged that PET equations,
13 especially in this climate change context, also rely on empirical coefficients which add
14 another source of uncertainty. Indeed, if different coefficients are selected for different
15 locations under current climate, it is conceivable that different coefficients would also be
16 appropriate for possible future climates in a catchment. This analysis could be extended
17 on future work on this subject, as for example applied in Kay *et al.* (2013). Only lumped
18 conceptual hydrological models were explored, mainly to limit implementation and
19 computation time as well as parameter identification issues, but inclusion of several other
20 model classes would be an important complementary contribution. Finally, uncertainties
21 associated to snow modules turned out small for the current climate period as well as for
22 the projections. It should be mentioned that the selected tools originated from the sane
23 snow module (CemaNeige) re-designed in six other versions and that this approach may
24 have affected the results. Here also, more diverse modules may be considered in further
25 exploration of this issue.

26

27 **5 Acknowledgements**

28 The authors acknowledge NSERC, Ouranos, and Hydro-Québec for support, as well as
29 partners in the QBIC³ (Quebec-Bavaria International Collaboration on Climate Change)
30 project. We also thank the reviewers for their discussions, comments, and references.

1

2 **6 References**

3 Allen, R. G., Walter, I. A., Elliott, R., Howell, T., Itenfisu, D. and Jensen, M.: The ASCE
4 standardized reference Evapotranspiration equation, 2005.

5 Bae, D. H., Jung, I. W. and Lettenmaier, D. P.: Hydrologic uncertainties in climate
6 change from IPCC AR4 GCM simulations of the Chungju Basin, Korea, *J. Hydrol.*,
7 401(1-2), 90–105, 2011.

8 Bergström, S. and Forsman, A.: Development of a conceptual deterministic rainfall-
9 runoff model, *Nord. Hydrol.*, 4(3), 147–170, 1973.

10 Beven, K. J. and Kirkby, M. J.: A physically based variable contributing area model of
11 basin hydrology, *Hydrol. Sci. Bull.*, 24(1), 43–69, 1979.

12 Boé, J., Terray, L., Martin, E. and Habets, F.: Projected changes in components of the
13 hydrological cycle in French river basins during the 21st century, *Water Resour. Res.*,
14 45(8), 1–15, 2009.

15 Bormann, H.: Sensitivity analysis of 18 different potential evapotranspiration models to
16 observed climatic change at German climate stations, *Clim. Change*, 104(3-4), 729–753,
17 doi:10.1007/s10584-010-9869-7, 2011.

18 Boucher, M.-A., Perreault, L. and Anctil, F.: Tools for the assessment of hydrological
19 ensemble forecasts obtained by neural networks, *J. Hydroinformatics*, 11(3–4), 297–307,
20 doi:10.2166/hydro.2009.037, 2009.

21 Boyer, C., Chaumont, D., Chartier, I. and Roy, A. G.: Impact of climate change on the
22 hydrology of St. Lawrence tributaries, *J. Hydrol.*, 384(1-2), 65–83,
23 doi:10.1016/j.jhydrol.2010.01.011, 2010.

24 Burnash, R. J. C., Ferral, R. L. and McGuire, R. A.: A general streamflow simulation
25 system : Conceptual modeling for digital computers, 1973.

1 Carter, T., Hulme, M. and Viner, D.: Representing uncertainty in climate change
2 scenarios and impact studies, in Proceedings of the ECLAT-2 Helsinki Workshop, p.
3 128., 1999.

4 Chiew, F. H. S. and McMahon, T. A.: Application of the daily rainfall-runoff model
5 MODHYDROLOG to 28 Australian catchments, *J. Hydrol.*, 153(1-4), 383–416, 1994.

6 Chiew, F. H. S. and Siriwardena, L.: Estimation of SIMHYD parameter values for
7 application in ungauged catchments, in MODSIM 2005 International Congress on
8 Modelling and Simulation, pp. 2883–2889, Modelling and Simulation Society of
9 Australia and New Zealand, Melbourne, Australia, 2005.

10 Cormary, Y. and Guilbot, A.: Étude des relations pluie-débit sur trois bassins versants
11 d’investigation, in IAHS Publication No.108 - Madrid Symposium, pp. 265–279,
12 Madrid., 1973.

13 Deser, C., Knutti, R., Solomon, S. and Phillips, A. S.: Communication of the role of
14 natural variability in future North American climate, *Nat. Clim. Chang.*, 2(October), 775–
15 780, doi:10.1038/NCLIMATE1562, 2012.

16 Dettinger, M. D.: From climate-change spaghetti to climate-change distributions for 21st
17 Century California, *San Fr. Estuary Watershed Sci.*, 3(1), 1–14, 2005.

18 Duan, Q. and Gupta, V.: Effective and efficient global optimization for conceptual
19 rainfall-runoff models, *Water Resour.*, 28(4), 1015–1031, 1992.

20 Duan, Q., Sorooshian, S. and Gupta, V.: Optimal use of the SCE-UA global optimization
21 method for calibrating watershed models, *J. Hydrol.*, 158, 265–284, 1994.

22 De Elía, R. and Côté, H.: Climate and climate change sensitivity to model configuration
23 in the Canadian RCM over North America, *Meteorol. Zeitschrift*, 19(4), 325–339,
24 doi:10.1127/0941-2948/2010/0469, 2010.

25 Fortin, V. and Turcotte, R.: Le modèle hydrologique MOHYSE, Quebec city., 2007.

26 Franz, K. J., Butcher, P. and Ajami, N. K.: Addressing snow model uncertainty for
27 hydrologic prediction, *Adv. Water Resour.*, 33(8), 820–832, 2010.

1 Garçon, R.: Modèle global pluie-débit pour la prévision et la prédétermination des crues,
2 La Houille Blanche, 7(8), 88–95, 1999.

3 Gardner, L. R.: Assessing the effect of climate change on mean annual runoff, *J. Hydrol.*,
4 379(3-4), 351–359, doi:10.1016/j.jhydrol.2009.10.021, 2009.

5 Girard, G., Morin, G. and Charbonneau, R.: Modèle précipitations-débits à discrétisation
6 spatiale, *Cah. ORSTOM, Série Hydrol.*, IX(4), 35–52, 1972.

7 Görgen, K., Beersma, J., Brahmer, G., Buiteveld, H., Carambia, M., de Keizer, O., Krahe,
8 P., Nilson, E., Lammersen, R., Perrin, C. and Volken, D.: Assessment of climate change
9 impacts on discharge in the Rhine river basin : Results of the RheinBlick2050 project.,
10 2010.

11 Jakeman, A. J., Littlewood, I. G. and Whitehead, P. G.: Computation of the instantaneous
12 unit hydrograph and identifiable component flows with application to two small upland
13 catchments, *J. Hydrol.*, 117, 275–300, 1990.

14 Jung, I. W., Bae, D. H. and Lee, B. J.: Possible change in Korean streamflow seasonality
15 based on multi-model climate projections, *Hydrol. Process.*, 13, doi:10.1002/hyp.9215,
16 2012.

17 Kay, A. L. and Davies, H. N.: Calculating potential evaporation from climate model data:
18 A source of uncertainty for hydrological climate change impacts, *J. Hydrol.*, 358(3-4),
19 221–239, doi:10.1016/j.jhydrol.2008.06.005, 2008.

20 Kay, A. L., Davies, H. N., Bell, V. A., Jones, R. G.: Comparison of uncertainty sources
21 for climate change impacts: flood frequency in England, *Clim. Change*, 92, 41–63, doi:
22 10.1007/s10584-008-9471-4, 2009.

23 Kay, A. L., Bell, V. A., Blyth, E. M., Crooks, S. M., Davies, H. N. and Reynard, N. S.: A
24 hydrological perspective on evaporation: historical trends and future projections in
25 Britain, *J. Water Clim. Chang.*, 4(3), 193–208, doi:10.2166/wcc.2013.014, 2013.

26 Kiparsky, M. and Gleick, P. H.: Climate change and California water resources, in *The*
27 *World's water 2004-2005*, edited by P. H. Gleick, pp. 157–188, Island Press, Washington
28 D. C., 2004.

1 Ludwig, R., May, I., Turcotte, R., Vescovi, L., Braun, M., Cyr, J.-F., Fortin, L.-G.,
2 Chaumont, D. and Biner, S.: The role of hydrological model complexity and uncertainty
3 in climate change impact assessment, *Adv. Geosci.*, 21, 63–71, 2009.

4 Mathevet, T.: *Quels modèles pluie-débit globaux au pas de temps horaire ?*, 463 pp.,
5 École Nationale du Génie Rural, des Eaux et des Forêts., 2005.

6 Maurer, E. P.: Uncertainty in hydrologic impacts of climate change in the Sierra Nevada,
7 California, under two emissions scenarios, *Clim. Change*, 82(3-4), 309–325, 2007.

8 Mazenc, B., Sanchez, M. and Thiery, D.: Analyse de l'influence de la physiographie d'un
9 bassin versant sur les paramètres d'un modèle hydrologique global et sur les débits
10 caractéristiques à l'exutoire, *J. Hydrol.*, 69, 97–118, 1984.

11 Minville, M., Brissette, F. and Leconte, R.: Uncertainty of the impact of climate change
12 on the hydrology of a nordic watershed, *J. Hydrol.*, 358(1-2), 70–83, 2008.

13 Moore, R. J. and Clarke, R. T.: A Distribution Function Approach to Rainfall Runoff
14 Modeling, *Water Resour. Res.*, 17(5), 1367–1382, 1981.

15 Nakicenovic, N., Alcamo, J., Davis, G., de Vries, B., Fenhann, J., Gaffin, S., Gregory, K.,
16 Grübler, A., Jung, T. Y., Kram, T., Lebre La Rovere, E., et al.: Emissions Scenarios. A
17 Special Report of Working Group III of the Intergovernmental Panel on Climate Change,
18 Cambridge University Press, Cambridge, U.K., 2000.

19 Nash, J. E. and Sutcliffe, J. V.: River flow forecasting through conceptual models. Part I -
20 A discussion of principles, *J. Hydrol.*, 10, 282–290, 1970.

21 Nicolle, P., Ramos, M.-H., Andréassian, V. and Valéry, A.: Mieux prévoir les crues
22 nivales : Évaluation de prévisions probabilistes de débit sur des bassins versants de
23 montagne français, in *Colloque SHF : "L'eau en montagne, mieux observer pour mieux
24 prévoir,"* pp. 163–17, Société Hydrotechnique de France, Lyon, France., 2011.

25 Nielsen, S. A. and Hansen, E.: Numerical simulation of the rainfall-runoff process on a
26 daily basis, *Nord. Hydrol.*, 4, 171–190, 1973.

27 O'Connell, P. E., Nash, J. E. and Farrell, J. P.: River flow forecasting through conceptual
28 models. Part II - The Brosna catchment at Ferbane, *J. Hydrol.*, 10, 317–329, 1970.

1 Oudin, L., Andréassian, V., Mathevet, T., Perrin, C. and Michel, C.: Dynamic averaging
2 of rainfall-runoff model simulations from complementary model parameterizations,
3 *Water Resour. Res.*, 42(7), 10, 2006.

4 Oudin, L., Hervieu, F., Michel, C., Perrin, C., Andréassian, V., Anctil, F. and Loumagne,
5 C.: Which potential evapotranspiration input for a lumped rainfall-runoff model? Part
6 2—Towards a simple and efficient potential evapotranspiration model for rainfall-runoff
7 modelling, *J. Hydrol.*, 303(1-4), 290–306, 2005.

8 Perrin, C., Michel, C. and Andréassian, V.: Does a large number of parameters enhance
9 model performance? Comparative assessment of common catchment model structures on
10 429 catchments, *J. Hydrol.*, 242(3-4), 275–301, 2001.

11 Perrin, C., Michel, C. and Andréassian, V.: Improvement of a parsimonious model for
12 streamflow simulation, *J. Hydrol.*, 279(1-4), 275–289, doi:10.1016/S0022-
13 1694(03)00225-7, 2003.

14 Poulin, A., Brissette, F., Leconte, R., Arsenault, R. and Malo, J.-S.: Uncertainty of
15 hydrological modelling in climate change impact studies in a Canadian, snow-dominated
16 river basin, *J. Hydrol.*, 409(3-4), 626–636, doi:10.1016/j.jhydrol.2011.08.057, 2011.

17 Prudhomme, C., Jakob, D. and Svensson, C.: Uncertainty and climate change impact on
18 the flood regime of small UK catchments, *J. Hydrol.*, 277(1-2), 1–23, 2003.

19 Quintana Seguí, P., Ribes, A., Martin, E., Habets, F. and Boé, J.: Comparison of three
20 downscaling methods in simulating the impact of climate change on the hydrology of
21 Mediterranean basins, *J. Hydrol.*, 383(1-2), 111–124, doi:10.1016/j.jhydrol.2009.09.050,
22 2010.

23 Schmidli, J., Frei, C. and Vidale, P.-L.: Downscaling from GCM precipitation: a
24 benchmark for dynamical and statistical downscaling methods, *Int. J. Climatol.*, 26(5),
25 679–689, doi:10.1002/joc.1287, 2006.

26 Scinocca, J. F., McFarlane, N. A., Lazare, M., Li, J. and Plummer, D.: Technical Note:
27 The CCCma third generation AGCM and its extension into the middle atmosphere,
28 *Atmos. Chem. Phys.*, 8(23), 7055–7074, doi:10.5194/acp-8-7055-2008, 2008.

1 Seiller, G., Anctil, F. and Perrin, C.: Multimodel evaluation of twenty lumped
2 hydrological models under contrasted climate conditions, *Hydrol. Earth Syst. Sci.*, 16(4),
3 1171–1189, doi:10.5194/hess-16-1171-2012, 2012.

4 Singh, V. P. and Xu, C.-Y.: Evaluation and Generalization of 13 Mass Transfer
5 Equations for Determining Free Water Evaporation, *Hydrol. Process.*, 11(3), 311–323,
6 1997.

7 Sugawara, M.: Automatic calibration of the tank model, *Hydrol. Sci. Bull.*, 24(3), 375–
8 388, 1979.

9 Teng, J., Vaze, J., Chiew, F. H. S., Wang, B. and Perraud, J.-M.: Estimating the Relative
10 Uncertainties Sourced from GCMs and Hydrological Models in Modeling Climate
11 Change Impact on Runoff, *J. Hydrometeorol.*, 13(1), 122–139, doi:10.1175/JHM-D-11-
12 058.1, 2012.

13 Thiery, D.: Utilisation d'un modèle global pour identifier sur un niveau piézométrique
14 des influences multiples dues à diverses activités humaines, *IAHS Publ. No.136*, 71–77,
15 1982.

16 Thornthwaite, C. W. and Mather, J. R.: *The Water Balance*. Publications in Climatology,
17 Vol. VIII, No. 1, 1955.

18 Valéry, A.: *Modélisation précipitations – débit sous influence nivale. Élaboration d'un*
19 *module neige et évaluation sur 380 bassins versants*, 417 pp., Agro Paris Tech., 2010.

20 Velázquez, J.-A., Anctil, F. and Perrin, C.: Performance and reliability of multimodel
21 hydrological ensemble simulations based on seventeen lumped models and a thousand
22 catchments, *Hydrol. Earth Syst. Sci. Discuss.*, 7(3), 4023–4058, 2010.

23 Velázquez, J.-A., Schmid, J., Ricard, S., Muerth, M. J., Gauvin St-Denis, B., Minville,
24 M., Chaumont, D., Caya, D., Ludwig, R. and Turcotte, R.: An ensemble approach to
25 assess hydrological models' contribution to uncertainties in the analysis of climate
26 change impact on water resources, *Hydrol. Earth Syst. Sci.*, 17(2), 565–578,
27 doi:10.5194/hess-17-565-2013, 2013.

- 1 Vicuna, S., Maurer, E. P., Joyce, B., Dracup, J. A. and Purkey, D.: The Sensitivity of
2 California Water Resources to Climate Change Scenarios, *J. Am. Water Resour. Assoc.*,
3 43(2), 482–498, doi:10.1111/j.1752-1688.2007.00038.x, 2007.
- 4 Wagener, T., Boyle, D. P., Lees, M. J., Wheater, H. S., Gupta, H. V. and Sorooshian, S.:
5 A framework for development and application of hydrological models, *Hydrol. Earth
6 Syst. Sci.*, 5(1), 13–26, doi:10.5194/hess-5-13-2001, 2001.
- 7 Wang, Y. C., Yu, P. S. and Yang, T. C.: Comparison of genetic algorithms and shuffled
8 complex evolution approach for calibrating distributed rainfall-runoff model, *Hydrol.
9 Process.*, 24(8), 1015–1026, doi:10.1002/hyp, 2009.
- 10 Warmerdam, P. M. M., Kole, J. and Chormanski, J.: Modelling rainfall-runoff processes
11 in the Hupselse Beek research basin, in *Ecohydrological processes in small basins,*
12 *Proceedings of the Strasbourg Conference (24-26 September 1996), IHP-V, Technical
13 Documents in Hydrology n°14, pp. 155–160, UNESCO, Paris, 1997.*
- 14 Wilks, D. S.: *Statistical Methods in the Atmospheric Sciences: An introduction,*
15 *Academic press, 1995.*
- 16 Xu, C.-Y. and Singh, V. P.: Dependence of evaporation on meteorological variables at
17 different time-scales and intercomparison of estimation methods, *Hydrol. Process.*, 12,
18 429–442, 1998.
- 19 Xu, C.-Y. and Singh, V. P.: Evaluation and generalization of radiation-based methods for
20 calculating evaporation, *Hydrol. Process.*, 14(2), 339–349, doi:10.1002/1099-1085, 2000.
- 21 Xu, C.-Y. and Singh, V. P.: Evaluation and generalization of temperature-based methods
22 for calculating evaporation, *Hydrol. Process.*, 15(2), 305–319, doi:10.1002/hyp.119,
23 2001.
- 24 Xu, C.-Y. and Singh, V. P.: Cross comparison of empirical equations for calculating
25 potential evapotranspiration with data from Switzerland, *Water Resour. Manag.*, 16, 197–
26 219, 2002.
- 27 Zhao, R. J., Zuang, Y. L., Fang, L. R. and Zhang, Q. S.: The Xinanjiang model, *IAHS
28 Publ. No.129, 351–356, 1980.*

29

1 Table 1 – List of the twenty lumped conceptual models and their source of inspiration

Name	Acronym	Free parameters	Storages	Derived from
M01	BUCK	6	3	BUCKET (Thorntwaite et Mather, 1955)
M02	CEQU	9	2	CEQUEAU (Girard et al., 1972)
M03	CRE0	6	3	CREC (Cormary et Guilbot, 1973)
M04	GARD	6	3	GARDENIA (Thiery, 1982)
M05	GR4J	4	3	GR4J (Perrin et al., 2003)
M06	HBV0	9	3	HBV (Bergström et al., 1973)
M07	HYMO	6	5	HYMOD (Wagener et al., 2001)
M08	IHAC	7	3	IHACRES (Jakeman et al., 1990)
M09	MART	7	4	MARTINE (Mazenc et al., 1984)
M10	MOHY	7	3	MOHYSE (Fortin et al., 2007)
M11	MORD	6	4	MORDOR (Garçon, 1999)
M12	NAM0	10	7	NAM (Nielsen et Hansen, 1973)
M13	PDM0	8	4	PDM (Moore et Clarke, 1981)
M14	SACR	9	5	SACRAMENTO (Burnash et al., 1973)
M15	SIMH	8	4	SIMHYD (Chiew et Siriwardena, 2005)
M16	SMAR	8	4	SMARY et SMARG (O'Connell et al., 1970)
M17	TAN0	7	4	TANK (Sugawara, 1979)
M18	TOPM	7	4	TOPMODEL (Beven et Kirkby, 1979)
M19	WAGE	8	3	WAGENINGEN (Warmerdam et al., 1997)
M20	XINA	8	5	XINANJIANG (Zhao et al., 1980)

2

- 1 Table 2 – List of the twenty-four PET formulations per category: combinational,
- 2 temperature-based, and radiation-based.

PET Class	Short name	Formulation name	Required data
Combinational	E01	Penman	RH, T, U, Rs
	E02	Penman-Monteith	RH, T, U, Rs
	E03	FAO56 P-M (ASCE)	RH, T, U, Rs
	E04	Priestley-Taylor	T, Rs
	E05	Kimberly-Penman	RH, T, U, Rs
	E06	Thom-Oliver	RH, T, U, Rs
Temperature-based	E07	Thornthwaite	T
	E08	Blaney-Criddle	T, Rs
	E09	Hamon	T, Rs
	E10	Romanenko	RH, T
	E11	Linacre	RH, T
	E12	MOHYSE	T
	E13	Hydro-Québec (HSAMI)	T
	E14	Kharrufa	T
Radiation-based	E15	Wendling (WASIM)	T, Rs
	E16	Turc	RH, T, Rs
	E17	Jensen-Haise	T
	E18	McGuinness-Bordne	T
	E19	Hargreaves	T
	E20	Doorenbos-Pruitt	RH, T, U, Rs
	E21	Abtew	RH, T, Rs
	E22	Makkink	T
	E23	Oudin	T
	E24	Baier-Robertson	T

with RH: relative humidity ; T: temperature ; U: wind speed ; Rs: incoming solar radiation

- 3
- 4

1 Table 3 – List of the seven snow module versions and free-parameters

Name	Free parameters	Version details
N1	2	Initial CemaNeige version (Valéry, 2010) P1: C_{Tg} ; P2: K_f
N2	4	Modified version (sinusoidal K_f , $T_f = -1^\circ\text{C}$, modified SnowFrac function, eT_G depending on air temp., progressive melt, free TG_{thresh}) P1: C_{Tg} ; P2: min K_f ; P3: max K_f ; P4: TG_{thresh}
N3	5	Modified version (linear SnowFrac with free parameters added, free thermal coeff C_t) P1: CoeffG ; P2: K_f ; P3: C_t ; P4: int ; P5: T_{50}
N4	4	Modified version (modified SnowFrac function, free thermal coeff C_t , free G_{thresh}) P1: C_{Tg} ; P2: K_f ; P3: C_t ; P4: G_{thresh}
N5	5	Modified version ($T_f = -1^\circ\text{C}$, sinusoidal K_f , modified SnowFrac function, free thermal coeff C_t , eT_G depending on air temp., progressive melt, free TG_{thresh}) P1: C_{Tg} ; P2: min K_f ; P3: max K_f ; P4: C_t ; P5: TG_{thresh}
N6	1	Modified version (modified SnowFrac function, eT_G not used) P1: K_f
N7	2	Modified version (50 layers, sinusoidal K_f , modified SnowFrac function) P1: C_{Tg} ; P2: K_f

2

3

- 1 Table 4 – Characteristics of the calibration performance (NSE_{sqrt}) pooled by hydrological
 2 models, PET formulations, and snow modules. Green color corresponds to the best
 3 performing options, when red color is the worst option

Hydrological model		PET formulation		Snow module	
Name	Median (5 th , 95 th)	Name	Median (5 th ,95 th)	Name	Median (5 th ,95 th)
M01	0.76 (0.67, 0.79)	E01	0.76 (0.56, 0.80)	N1	0.75 (0.53, 0.81)
M02	0.56 (0.48, 0.62)	E02	0.70 (0.50, 0.78)	N2	0.75 (0.53, 0.81)
M03	0.78 (0.70, 0.80)	E03	0.75 (0.55, 0.79)	N3	0.75 (0.55, 0.81)
M04	0.77 (0.68, 0.79)	E04	0.76 (0.58, 0.81)	N4	0.75 (0.55, 0.80)
M05	0.81 (0.72, 0.83)	E05	0.76 (0.55, 0.80)	N5	0.75 (0.52, 0.80)
M06	0.76 (0.69, 0.78)	E06	0.75 (0.56, 0.79)	N6	0.75 (0.56, 0.80)
M07	0.60 (0.49, 0.63)	E07	0.77 (0.60, 0.82)	N7	0.71 (0.52, 0.79)
M08	0.71 (0.64, 0.75)	E08	0.68 (0.47, 0.78)		
M09	0.76 (0.64, 0.80)	E09	0.76 (0.53, 0.81)		
M10	0.73 (0.58, 0.81)	E10	0.67 (0.49, 0.72)		
M11	0.74 (0.63, 0.80)	E11	0.74 (0.54, 0.80)		
M12	0.71 (0.36, 0.78)	E12	0.66 (0.45, 0.79)		
M13	0.57 (0.47, 0.65)	E13	0.77 (0.58, 0.81)		
M14	0.78 (0.68, 0.81)	E14	0.77 (0.61, 0.81)		
M15	0.75 (0.62, 0.79)	E15	0.75 (0.56, 0.79)		
M16	0.78 (0.68, 0.80)	E16	0.76 (0.58, 0.81)		
M17	0.76 (0.68, 0.80)	E17	0.75 (0.56, 0.80)		
M18	0.77 (0.67, 0.80)	E18	0.77 (0.59, 0.80)		
M19	0.76 (0.65, 0.81)	E19	0.75 (0.56, 0.81)		
M20	0.63 (0.56, 0.65)	E20	0.72 (0.54, 0.80)		
		E21	0.69 (0.49, 0.76)		
		E22	0.77 (0.57, 0.81)		
		E23	0.78 (0.59, 0.82)		
		E24	0.77 (0.59, 0.82)		

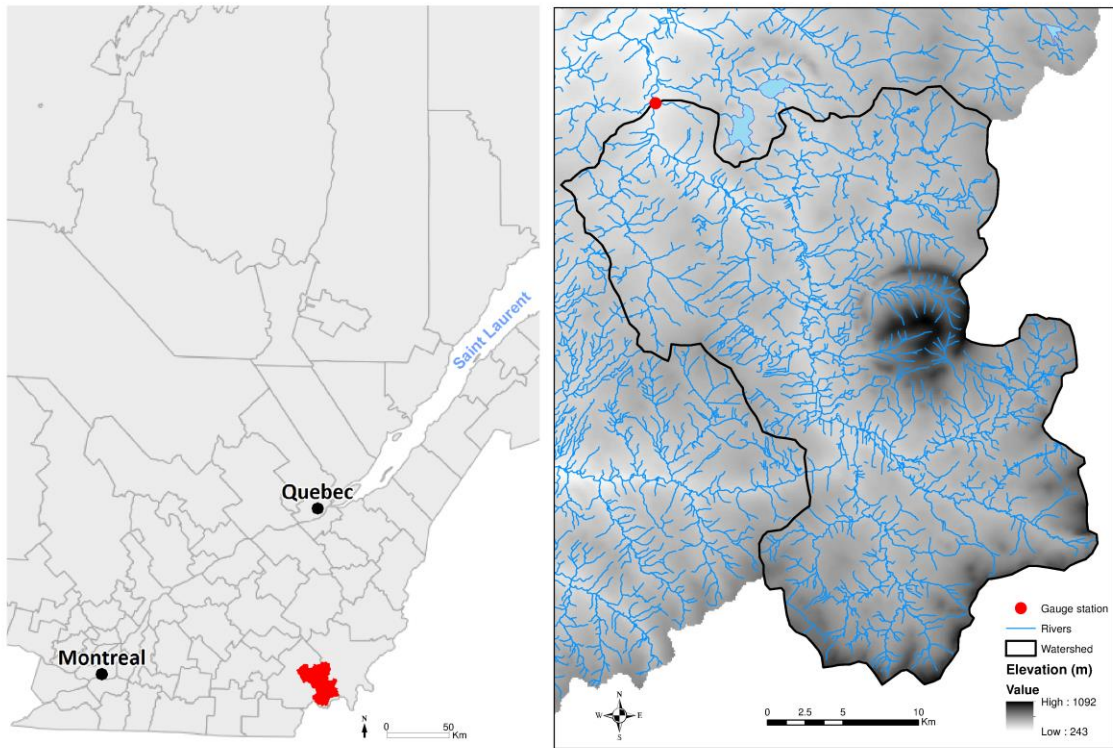
4

1 Table 5 – Characteristics of the median OMF relative change for different processes and
 2 periods

	Lowest value	Highest value	Standard deviation
OMF			
Hydrological model	+6.3 % (M02)	+16.8 % (M08)	2.4 %
PET formulation	+4.1 % (E13)	+17.1 % (E21)	3.3 %
Snow module	+9.1 % (N2)	+9.9 % (N3)	0.3 %
Climatic member	+2.7 % (C4)	+19.1 % (C3)	6.9 %
April to October OMF			
Hydrological model	-14.2 % (M06)	-4.1 % (M08)	2.4 %
PET formulation	-15.8 % (E14)	-1.7 % (E21)	3.1 %
Snow module	-11.3 % (N1)	-10.1 % (N6)	0.5 %
Climatic member	-19.5 % (C2)	-2.4 % (C3)	7.6 %
November to May OMF			
Hydrological model	+17.1 % (M17)	+27.5 % (M08)	2.1 %
PET formulation	+14.1 % (E14)	+32.2 % (E21)	4.0 %
Snow module	+20.5 % (N1)	+21.1 % (N6)	0.3 %
Climatic member	+15.7 % (C4)	+26.3 % (C3)	4.7 %

3

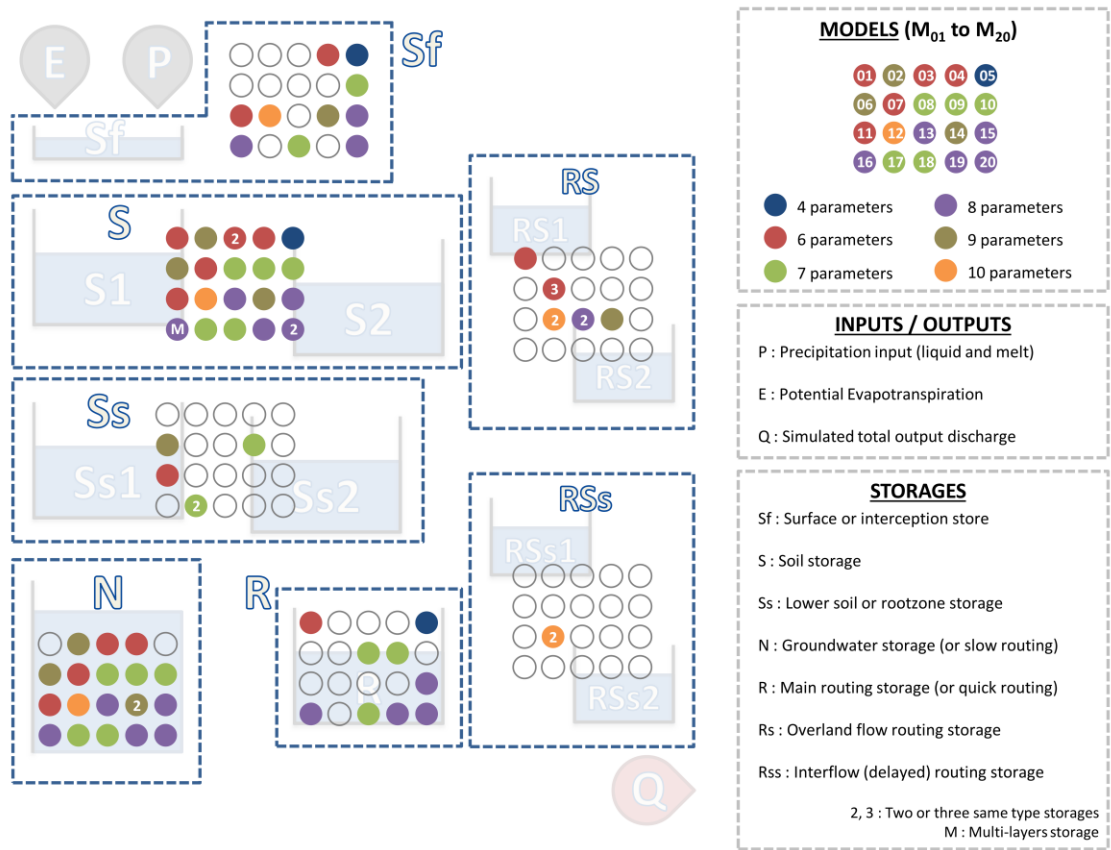
4



1

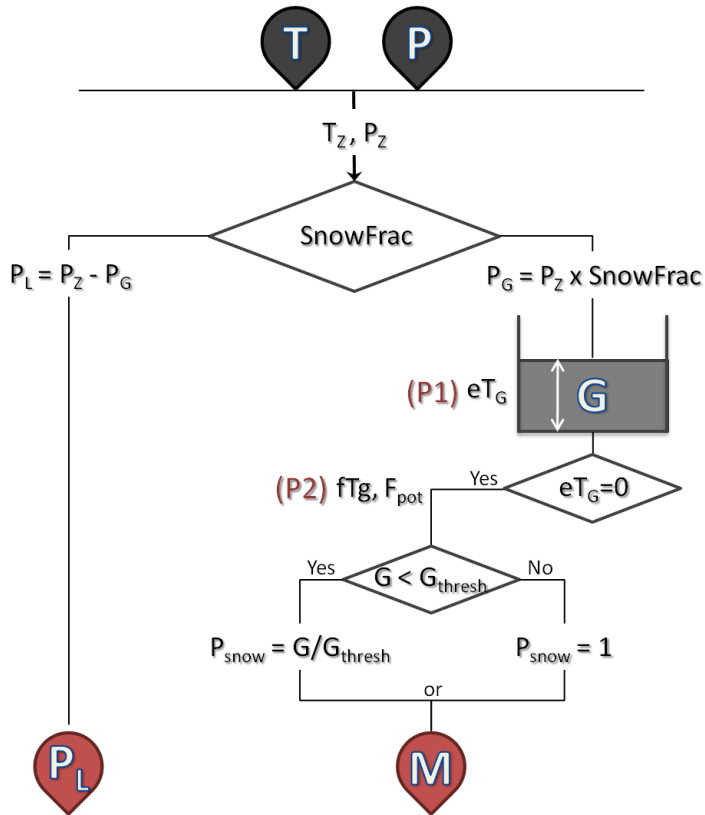
2 Figure 1: Localisation of the *au Saumon* catchment (738 km²; Canada)

3



1
 2
 3

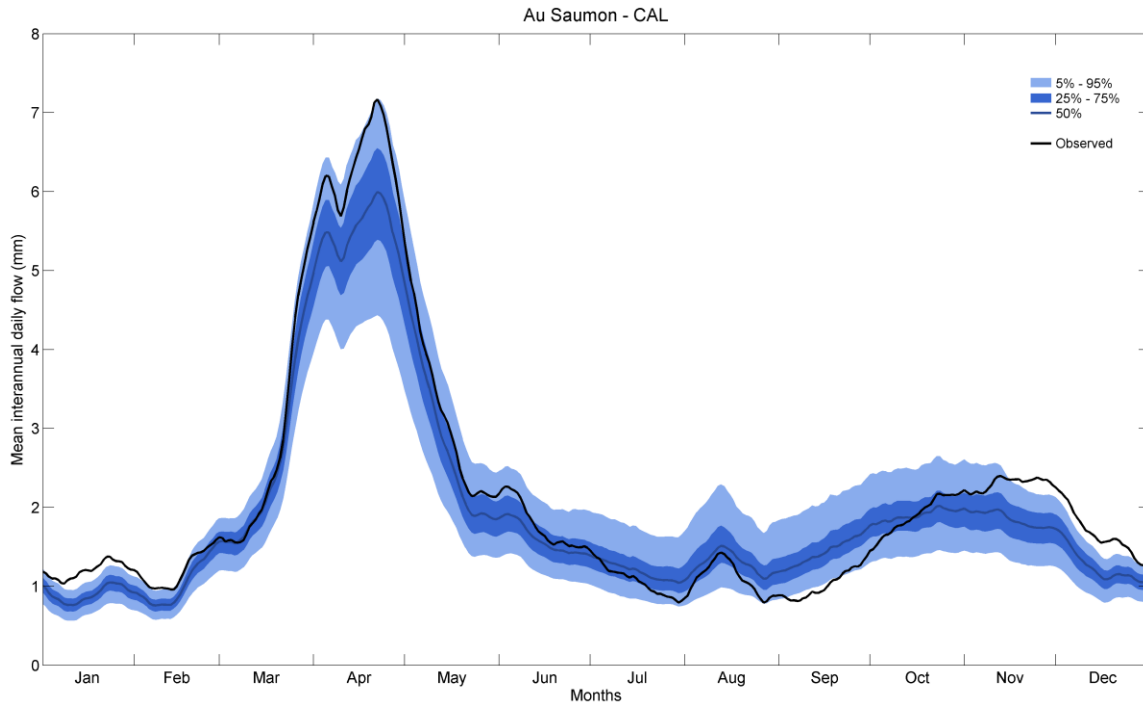
Figure 2: Illustration of the structural diversity of the twenty lumped conceptual models



1

2 Figure 3: Initial version of the CemaNeige snow module (N1). T is temperature, P is total
 3 precipitation, P_L is liquid precipitation, P_G is solid precipitation, and M is snowmelt. G
 4 corresponds to the snowpack and P1 and P2 are the two free parameters. (Modified from
 5 Valéry, 2010)

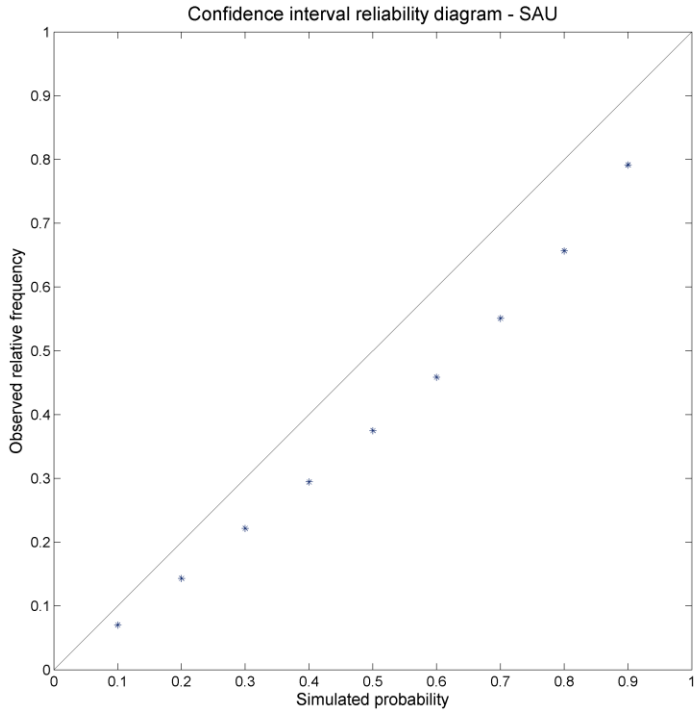
6



1

2 Figure 4: Cumulative uncertainties for the observed period simulation. The black line is
 3 the observed flow, the blue line depicts the median flow simulation, and the pale and dark
 4 blue envelopes, the distribution of the streamflow ensemble (5 % to 95% and 25 % to 75
 5 %, respectively).

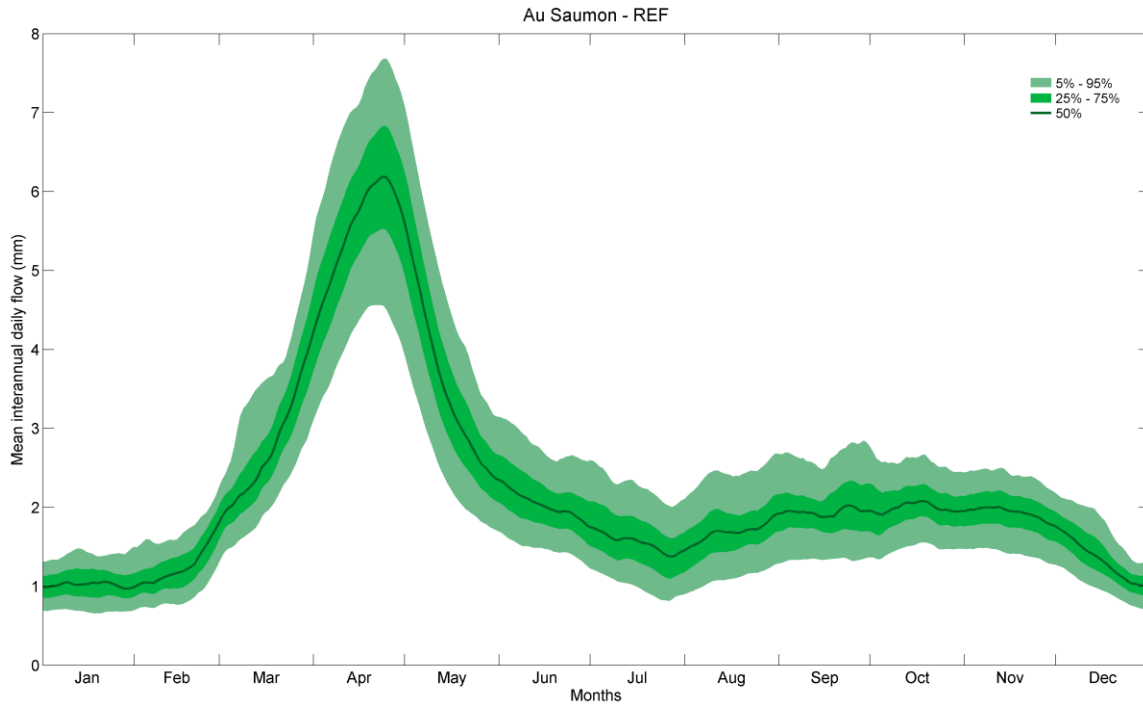
6



1

2 Figure 5: Confidence interval reliability diagram opposing simulated probability (x-axis)
3 and observed relative frequency (y-axis)

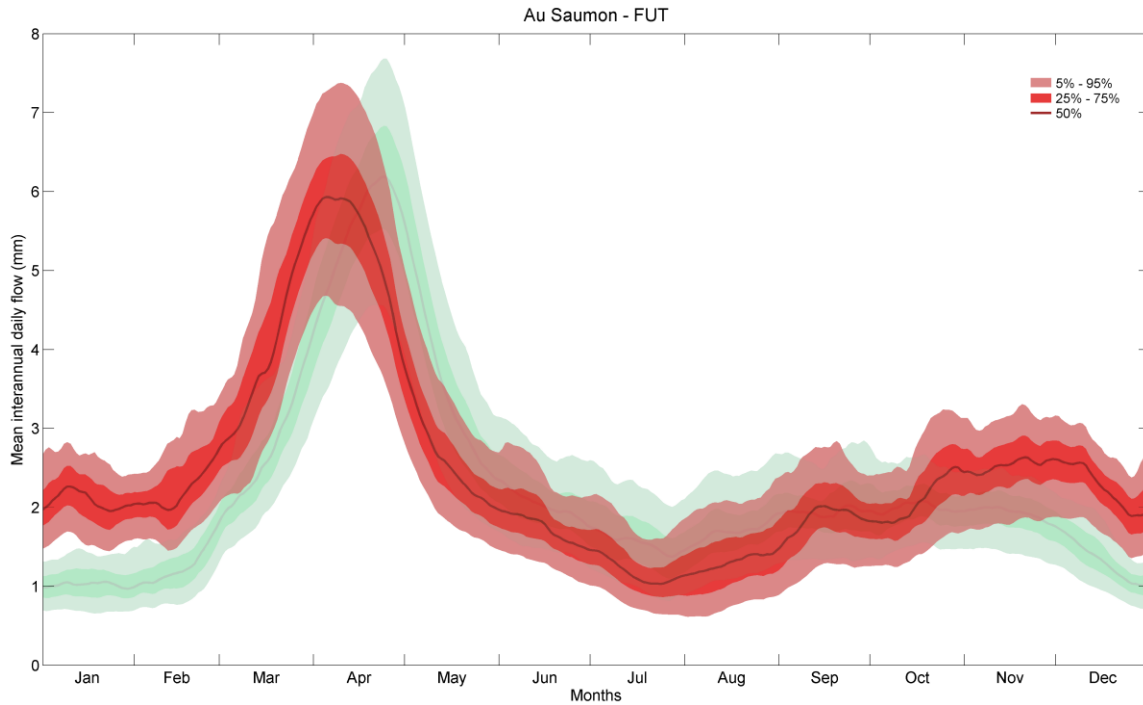
4



1

2 Figure 6: Cumulative uncertainties of the reference (REF) simulations. The line depicts
3 the median flow simulation and the pale and dark green envelopes, the distribution of the
4 streamflow ensemble (5 % to 95% and 25 % to 75 %, respectively).

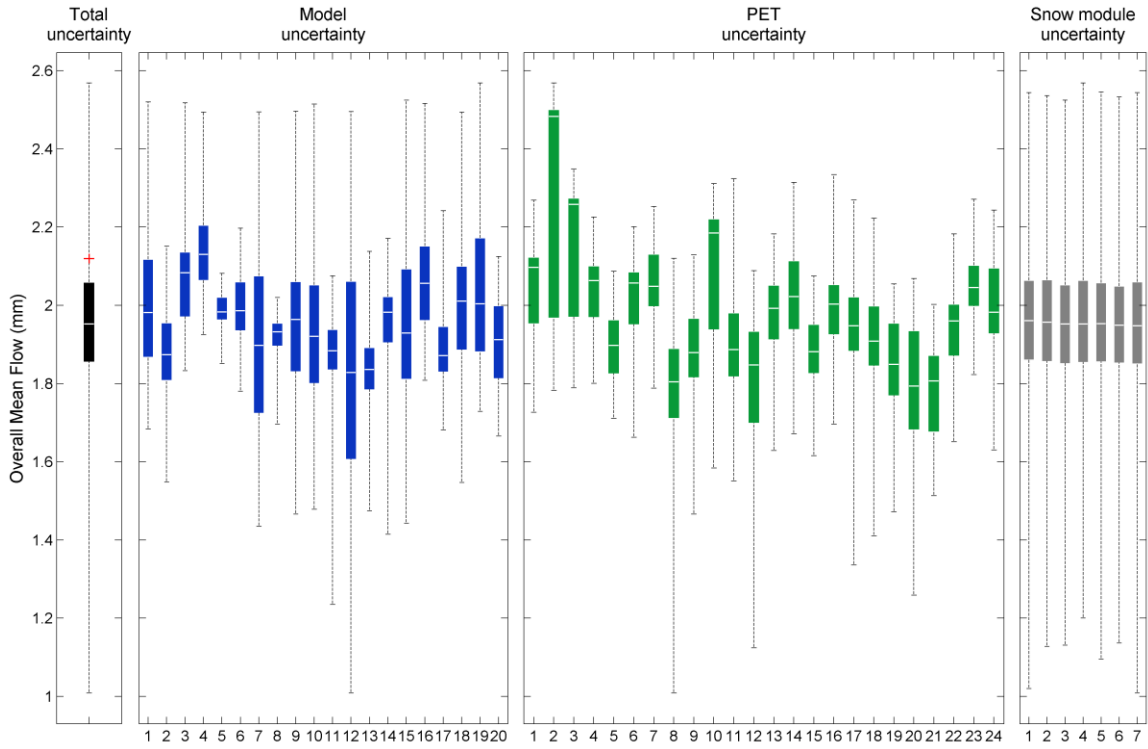
5



1

2 Figure 7: Cumulative uncertainties of the future (FUT) projection. The line depicts the
 3 median flow projection and the pale and dark red envelopes, the distribution of the
 4 streamflow ensemble (5 % to 95% and 25 % to 75 %, respectively). REF simulation is
 5 displayed transparently in green color.

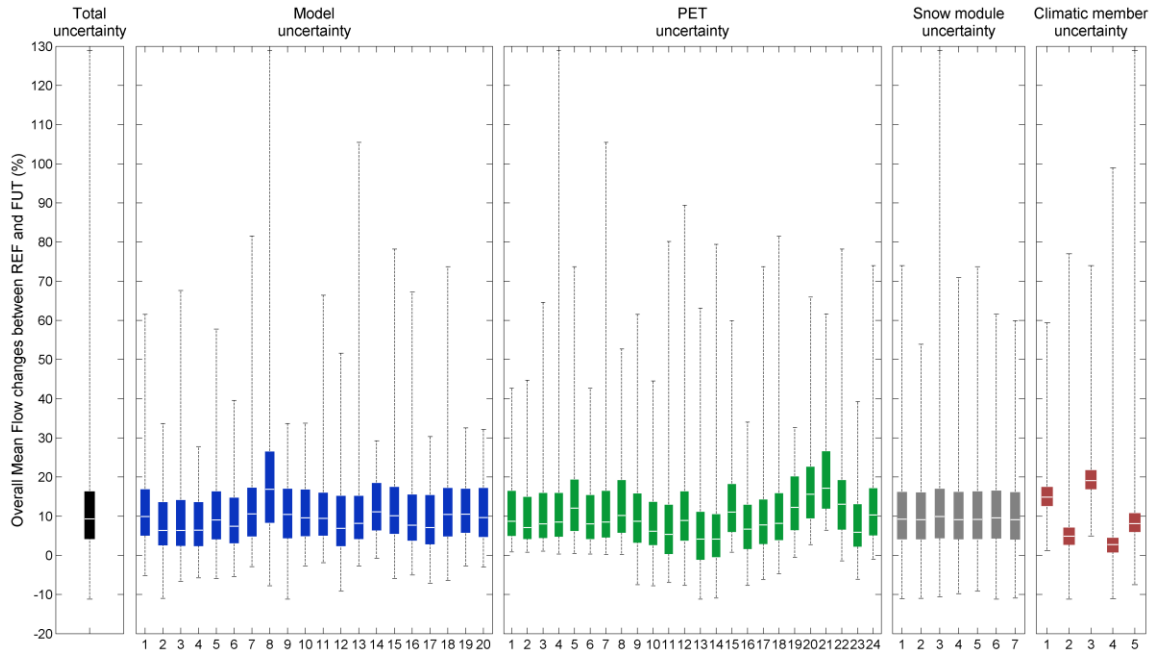
6



1

2 Figure 8: Total (black boxplot) and process-based overall mean flow (OMF, mm)
 3 uncertainty, for simulation on the observed period. The observed OMF is illustrated by a
 4 red cross in the total uncertainty box. Blue boxplots correspond to the lumped conceptual
 5 hydrological models, green boxplots to the PET formulations and grey boxplots to the
 6 snow modules.

7



1

2 Figure 9: Total (black boxplot), process-based, and climate overall mean flow evolution
 3 (from REF to FUT, %) uncertainty. Blue boxplots correspond to the lumped conceptual
 4 hydrological models, green boxplots to the PET formulations, grey boxplots to the snow
 5 modules and red boxplots to the climatic members.

6